

Optical orbital angular momentum from the curl of polarization

Xi-Lin Wang (汪喜林),¹ Jing Chen,¹ Yongnan Li (李勇男),¹ Jianping Ding (丁剑平),²
Cheng-Shan Guo (国承山),¹ and Hui-Tian Wang (王慧田)^{1,2,*}

¹*School of Physics and Key Laboratory of Weak-Light Nonlinear Photonics, Nankai University, Tianjin 300071, China*

²*Nanjing National Laboratory of Microstructures, Nanjing University, Nanjing 210093, China*

(Received 22 June 2010; published 13 December 2010)

We predict a new category of optical orbital angular momentum that is associated with the curl of polarization and a kind of vector field with radial-variant hybrid states of polarization that can carry such novel optical orbital angular momentum. We present a scheme for creating the desired vector fields. Optical trapping experiments validate that the vector fields, which have no additional phase vortex, exert torques to drive the orbital motion of the trapped isotropic microspheres.

DOI: 10.1103/PhysRevLett.105.253602

PACS numbers: 42.50.Tx, 03.50.Kk, 42.25.Ja, 42.50.Wk

A light field can carry spin angular momentum (SAM) or orbital angular momentum (OAM). As an intrinsic part of the nature of a light field, SAM is associated with circular polarization and has two possible quantized values of $\pm\hbar$ [1]. Since the original concept of optical OAM was pioneered by Allen *et al.* in 1992 [2], as a fundamentally new optical degree of freedom [3], OAM has attracted extensive attention and academic interest due to its practical and potential applications in various realms (such as nonlinear optics [4], atom optics [5], quantum optics and information [6], optical communication [7], optical tweezers and micromechanics or microfluidics [8], biosciences [8], and even astronomy [9]). The concept of the optical OAM has now been extended to other natural waves such as a radio wave [10], sonic wave [11], x ray [12], electron beam [13], and a matter wave [14], so that the optical OAM is undoubtedly an extensively interesting issue.

As predicted by Allen *et al.* in 1992 [2], a scalar vortex field with a helicoidal phase front of $\exp(-j\ell\phi)$ could carry an optical OAM of $\ell\hbar$ [1–3, 15–21]. Evidently, for scalar fields with homogeneous distribution of states of polarization (SoPs), the space-variant phase is a prerequisite for possibility of producing optical OAM caused by the phase. The question is whether the polarization as a fundamental nature of light can also be used to produce optical OAM. It is imaginable that the light fields with the space-variant distribution of SoPs have the possibility of carrying OAM. Consequently, vector fields with space-variant distribution of SoPs [22–25] offer an opportunity of producing optical OAM associated with the polarization nature.

In this Letter, we predict in theory and validate in experiment a new class of optical OAM associated with the curl of polarization independent of phase. It is quite different from the well-known OAM associated with the phase gradient independent of polarization. The theoretical result reveals that this novel OAM can be carried by a radial-variant vector field with hybrid SoPs. We present a scheme for creating the desired vector fields. An optical trapping experiment confirms that the optical OAM carried

by the vector fields we presented drives the motion of trapped isotropic microspheres around the ring focus. The present result is a breakthrough from the limitation that the polarization nature of light field can only influence optically anisotropic materials.

Theoretical Prediction.—A light field at an angular frequency ω has a vector potential \mathbf{A} , as $\mathbf{A}(x, y) = A(x, y) \times [\alpha(x, y)\hat{\mathbf{e}}_x + \beta(x, y)\hat{\mathbf{e}}_y] \exp(jkz - j\omega t)$ with $|\alpha|^2 + |\beta|^2 = 1$, where the complex amplitude A can be described by real-valued module u and phase ψ . α and β indicate the distribution of SoPs of a light field. Under the paraxial limit and the Lorenz gauge, the cycle-average momentum flux \mathbf{P} can be written as $\mathbf{P} \propto \langle \mathbf{E} \times \mathbf{H} \rangle$ in terms of the magnetic field $\mathbf{H} = (\nabla \times \mathbf{A}) / \mu_0$ and the electric field $\mathbf{E} = j\omega\mathbf{A} + j(\omega/k^2)\nabla(\nabla \cdot \mathbf{A})$. The transversal component of \mathbf{P} is divided into

$$\mathbf{P}_{\perp}^{(1)} \propto 2u^2 \nabla \psi, \quad (1a)$$

$$\mathbf{P}_{\perp}^{(2)} \propto ju^2(\alpha \nabla \alpha^* - \alpha^* \nabla \alpha + \beta \nabla \beta^* - \beta^* \nabla \beta), \quad (1b)$$

$$\mathbf{P}_{\perp}^{(3)} \propto j\nabla \times [u^2(\alpha\beta^* - \alpha^*\beta)\hat{\mathbf{e}}_z]. \quad (1c)$$

The cross product of \mathbf{P} with \mathbf{r} (radius vector) gives the angular momentum flux $\mathbf{J} \propto \mathbf{r} \times \mathbf{P}$. Accordingly, the z component of \mathbf{J} , J_z , is composed of three parts

$$J_z^{(1)} \propto 2u^2 \partial \psi / \partial \phi, \quad (2a)$$

$$J_z^{(2)} \propto ju^2(\alpha \partial \alpha^* / \partial \phi + \beta \partial \beta^* / \partial \phi - \text{c.c.}), \quad (2b)$$

$$J_z^{(3)} \propto jr \partial [u^2(\alpha\beta^* - \alpha^*\beta)] / \partial r. \quad (2c)$$

where $J_z^{(1)}$ is the well-known OAM associated with the azimuthal phase gradient, $J_z^{(2)}$ and $J_z^{(3)}$ are associated with the distribution of SoPs. If α and β are real valued, implying that SoP at any location of the field section is local linearly polarized, both $J_z^{(2)}$ and $J_z^{(3)}$ are zero. If either α or β is at least a complex-valued function, $J_z^{(2)}$ and $J_z^{(3)}$ are possibly nonzero values. $J_z^{(2)}$ arising from the azimuthal

variation of SoPs is the simple superposition of contributions from two orthogonal field components.

We are interested in $J_z^{(3)}$, a new class of optical OAM. We define a parameter σ , describing SoP, as $\sigma = j(\alpha\beta^* - \alpha^*\beta)$. For instance, $\sigma = +1$ or -1 represents the right-handed (RH) or left-handed (LH) circular polarization, whereas $\sigma = 0$ is the linear polarization. Surprisingly, $J_z^{(3)}$ originates from the *curl* of the vector $\sigma u^2 \hat{e}_z$. As we expected, the optical OAM can be indeed associated with space-variant SoPs independent of phase. To achieve nonzero-valued $J_z^{(3)}$, two prerequisites should be satisfied: (i) $\sigma \neq 0$, i.e., local SoPs at locations in the field section should not be all linearly polarized, and (ii) σ or SoPs should be radial-variant instead of being azimuthal-variant. A nonzero-valued $J_z^{(3)}$ requires the light field to be a vector field with the radial-variant hybrid SoPs. The crucial issue is how to create the desired vector field satisfying the above requirements.

We should emphasize that as a common requirement for light field carrying optical OAM, a certain physical quantity (phase or SoP) of light field must be space-variant. The helically phased scalar fields, which have on-axis phase singularity, carry the known OAM caused by the azimuthal phase gradient independent of polarization [see Eq. (2)]. In contrast, the radial-variant vector fields with hybrid SoPs, which have no polarization singularity, carry the optical OAM associated with the curl of polarization independent of phase [see Eq. (2c)].

Generation of Radial-Variant Vector Fields.—Most reported vector fields [22–32] have a common feature: the distribution of SoPs is a function of ϕ only. However, radial-variant vector fields are rarely involved. Niv *et al.* [33] reported the generation of radial-variant vector fields with space-variant axially symmetric distribution of SoPs with the aid of subwavelength grating for a 10.6 μm CO₂ laser. A crucial issue still remains: how to create the vector fields satisfying the requirements of producing the optical OAM associated with the curl of polarization. Based on the idea of wave-front reconstruction in the scheme presented in Refs. [24,25], the additional phase δ in the transmission function of a spatial light modulator (SLM) is a function of ϕ only, as $\delta = m\phi + \alpha_0$. The generated vector fields have the azimuthal-variant SoPs. In theory, if δ is a function of r only, as $\delta = 2n\pi r/r_0 + \alpha_0$ (where r_0 is the radius of the vector field, n is the radial index, and α_0 determines SoP at $r = 0$), the vector field should have radial-variant SoPs.

Generating the radial-variant vector field with local linear polarization requires a pair of orthogonal base vectors [24]. The scheme similar to Fig. 1 in Ref. [24] is shown by the dashed-line box in Fig. 3 below; in this situation two $\lambda/4$ wave plates are used to generate a pair of orthogonal RH and LH circularly polarized fields, and the additional phase in SLM is set as $\delta = 2n\pi r/r_0 + \alpha_0$. The intensity patterns of all generated vector fields exhibit uniform distribution and are indistinguishable for different values of n and α_0 . As shown in Figs. 1(a)–1(d), the intensity

patterns of four vector fields passing through a horizontal polarizer exhibit cylindrical symmetry with concentric extinction rings, suggesting that the SoPs of the generated vector fields have radial-variant and local linearly polarized distributions. The linear polarization at the center $r = 0$ is along the direction of $\phi = \alpha_0$.

We now generate the radial-variant vector fields with hybrid SoPs (including linear, elliptical, and circular polarizations). The scheme similar to Fig. 2 in Ref. [25] is shown by the dashed-line box in Fig. 3 below, in this situation two $\lambda/2$ wave plates are used to generate a pair of orthogonal linearly polarized fields, and the additional phase in SLM is still set as $\delta = 2n\pi r/r_0 + \alpha_0$. As shown in the 1st and 2nd columns of Fig. 2, the intensity patterns of two generated radial-variant vector fields exhibit the uniform distribution, although SoPs have hybrid distribution. As an example, in the 1st column, as r increases from $r = 0$ to r_0 , SoPs change from $\pi/4$ linear polarization at $r = 0$ to RH elliptical polarization within $r \in (0, r_0/4)$, RH circular polarization at $r = r_0/4$, RH elliptical polarization within $r \in (r_0/4, r_0/2)$, $3\pi/4$ linear polarization at $r = r_0/2$, LH elliptical polarization within $r \in (r_0/2, 3r_0/4)$, LH circular polarization at $r = 3r_0/4$, LH elliptical polarization within $r \in (3r_0/4, r_0)$, and finally, to $-3\pi/4$ linear polarization at $r = r_0$.

To characterize the distribution of SoPs of a vector field, three Stokes parameters, s_1 , s_2 , and s_3 , in the representation of the Poincaré sphere Σ should be specified [25,34]. For the radial-variant vector field with hybrid SoPs, the theoretical Stokes parameters are $s_1 = 0$, $s_2 = \cos(4n\pi r/r_0 + 2\alpha_0)$, and $s_3 = \sin(4n\pi r/r_0 + 2\alpha_0)$. The measured results, as shown in the 2nd to 4th rows of Fig. 2, exhibit cylindrical symmetry, implying that SoPs are indeed radial variant only as predicted in theory, $s_1 = 0$, so SoP at any location of the field section is represented by a point in the $\pi/2$ meridian circle on Σ . For instance, in the 1st column, the SoP at $r = 0$ is $\pi/4$ linearly polarized and is located at point $(s_1, s_2, s_3) = (0, 1, 0)$ in the equator on Σ , whereas the SoP at $r = r_0/4$ is RH circularly polarized and is located at the north pole of $(0, 0, 1)$ on Σ , and so on. For comparison, the measured Stokes parameters of the local linearly polarized vector field are also shown in the 3rd column of Fig. 2. Both theoretical and measured results show that this vector field has $s_3 = 0$, suggesting that the SoP at any location is indeed linearly polarized and is

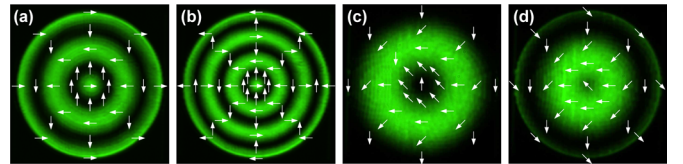


FIG. 1 (color online). Intensity patterns of four radial-variant linearly polarized vector fields passing through a horizontal polarizer and their schematics of SoPs. (a) $n = 1.0$ and $\alpha_0 = 0$, (b) $n = 1.5$ and $\alpha_0 = 0$, (c) $n = 0.5$ and $\alpha_0 = \pi/2$, and (d) $n = 0.5$ and $\alpha_0 = 3\pi/4$.

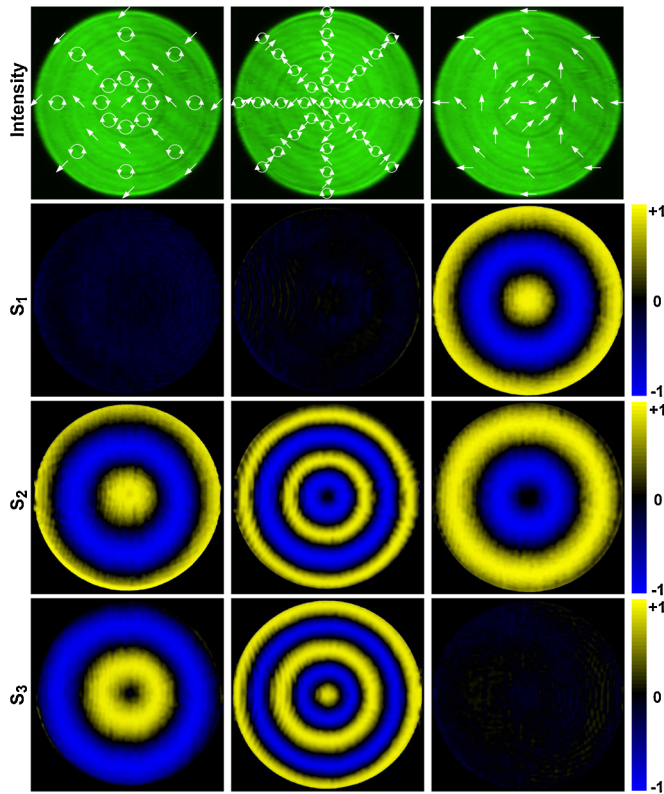


FIG. 2 (color online). Intensity patterns of two radial-variant vector fields with hybrid SoPs, schematics of SoPs, and measured Stokes parameters. The 1st and 2nd columns correspond to ($n = 0.5$, $\alpha_0 = 0$) and ($n = 1.0$, $\alpha_0 = \pi/4$), respectively. For comparison, a local linearly polarized vector field with ($n = 0.5$, $\alpha_0 = 0$) is also depicted in the 3rd column.

located at the equator on Σ . The generated radial-variant vector fields with hybrid SoPs indeed satisfy the two prerequisites previously mentioned for generating OAM associated with the curl of polarization.

Evidence of OAM Associated with the Curl of Polarization.—To confirm the feasibility of OAM associated with the curl of polarization, the focused vector field as an optical tweezer is a useful tool. Figure 3 shows the trapping experimental scheme, wherein the laser source at 532 nm has a power of 20 mW. All the generated vector fields have the same radius of $r_0 = 2.5$ mm, a $60\times$ objective (with $\text{NA} = 0.7$) is used to focus the vector field, and the neutral colloidal microspheres with a diameter of $3.2 \mu\text{m}$ are dispersed in a layer of sodium dodecyl sulfate solution between a glass coverslip and a microscope slide.

We first implement simulations for the focusing property of radial-variant vector fields. The parameters used in simulations are the same as those used in the experiment. The simulation results indicate that the radial-variant vector fields (not only local linear polarization but also hybrid SoPs) are tightly focused into a ring focus using a high NA objective. As an example, the simulated intensity pattern of the ring focus where $n = 10$ is shown in the inset (a) of Fig. 3. The inset (b) of Fig. 3 shows the simulated radial

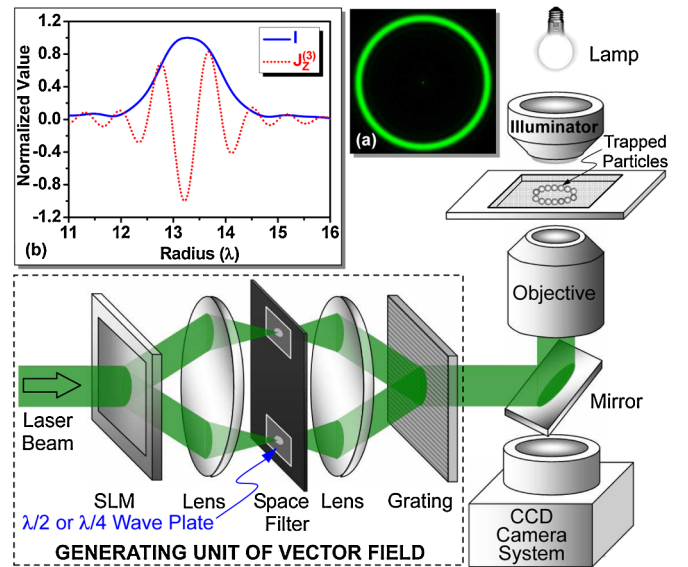


FIG. 3 (color online). Experimental configuration to validate OAM associated with the curl of polarization. The dashed-line box shows the generating unit of radial-variant vector fields. Inset (a) shows an example of simulated ring focus. Inset (b) shows the properties of the ring focus for a radial-variant vector field with hybrid SoPs ($n = 10$), where the solid and dashed lines are the radial dependences of intensity and OAM $J_z^{(3)}$, respectively.

dependences of intensity (solid line) and of OAM $J_z^{(3)}$ associated with the curl of polarization (dashed line) in the focal plane for the radial-variant vector field with hybrid SoPs where $n = 10$. The maximum OAM $J_z^{(3)}$ and the strongest intensity locate at the same radial position, which is of such great importance that trapped particles in the ring focus can acquire the maximum torque when rotating around the ring focus.

The trapping experiments indicate that the ring traps generated by radial-variant vector fields (not only with the local linear polarization but also with hybrid SoPs) can trap an arbitrary number of particles. The reason originates from the fact that the ring focus has a continuously changeable radius because n can be an arbitrary real number, which is quite different from the discrete radius of the ring focus generated by the azimuthal-variant vector field. For the particles trapped in the ring optical tweezers produced by radial-variant vector fields with local linear polarization, no motion is observed around the ring focus, implying that radial-variant vector fields with local linear polarization carry no optical OAM.

We are very interested in the trapping property of the ring traps generated by the radial-variant vector field with hybrid SoPs. As the time-lapse photographs shown in the upper row of Fig. 4, the trapped particles when $n = 10$ move clockwise around the ring focus [35], with an orbital period of ~ 8.4 s. When n is switched from positive ($n = 10$) to negative ($n = -10$), the motion direction of the trapped particles is synchronously reversed [35], as

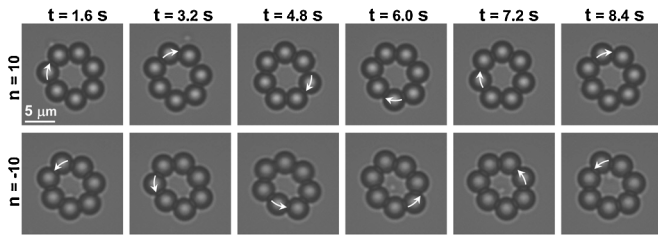


FIG. 4. Snapshots of the motion of trapped particles around the ring focus generated by radial-variant vector fields with hybrid SoPs, caused by polarization-curl-induced OAM (also see Ref. [35]).

shown in the bottom row of Fig. 4. The observed results imply that the ring traps have the capability to exert torque to the trapped isotropic particles. Consequently, the radial-variant vector fields with hybrid SoPs can carry the optical OAM associated with the curl of polarization independent of phase.

For the interaction of light with matter, the polarization can influence anisotropic materials, but not isotropic materials, which is true for scalar fields. As we predicted, the induction of the vector fields breaks this limitation to make the polarization nature of light field influence optically isotropic materials. Since SAM and OAM decouple in the paraxial limit [36] and SAM results in the rotation of an anisotropic particle around its own axis [21], our observed rotation of the trapped isotropic particles should be dominated by OAM.

Summary.—We predict a novel optical OAM associated with the curl of polarization independent of phase. To demonstrate this idea, a scheme is presented for creating the desired radial-variant vector fields and enabling the flexible generation of novel vector fields. Using optical traps, we confirm that the radial-variant vector fields with hybrid SoPs can carry this novel OAM, whereas the radial-variant linearly polarized vector fields cannot. Our results create a link between two important issues on optical OAM and vector field. Our idea may spur further independent insights into the generation of natural waves carrying OAM and the expansion of the functionality of many optical systems, thereby facilitating the development of additional surprising applications.

The authors acknowledge the support of NFSC under Grants No. 10934003 and No. 10874078, and 973 Program of China under Grant No. 2006CB921805.

*htwang@nankai.edu.cn/htwang@nju.edu.cn

- [1] M. Padgett, J. Courtial, and L. Allen, *Phys. Today* **57**, 5, 35 (2004); L. Allen, M. J. Padgett, and M. Babiker, *Prog. Opt.* **39**, 291 (1999).
 [2] L. Allen *et al.*, *Phys. Rev. A* **45**, 8185 (1992).
 [3] G. Molina-Terriza, J. P. Torres, and L. Torner, *Nature Phys.* **3**, 305 (2007).

- [4] See for example: D. N. Neshev *et al.*, *Phys. Rev. Lett.* **92**, 123903 (2004); N. K. Efremidis *et al.*, *Phys. Rev. Lett.* **98**, 113901 (2007); S. Feng and P. Kumar, *Phys. Rev. Lett.* **101**, 163602 (2008).
 [5] See for example: S. Barreiro and J. W. R. Tabosa, *Phys. Rev. Lett.* **90**, 133001 (2003); M. S. Bigelow, P. Zerom, and R. W. Boyd, *Phys. Rev. Lett.* **92**, 083902 (2004); M. F. Andersen *et al.*, *Phys. Rev. Lett.* **97**, 170406 (2006).
 [6] See for example: A. Mair *et al.*, *Nature (London)* **412**, 313 (2001); A. R. Altman *et al.*, *Phys. Rev. Lett.* **94**, 123601 (2005); J. E. Nagali *et al.*, *Nat. Photon.* **3**, 720 (2009); Leach *et al.*, *Science* **329**, 662 (2010).
 [7] C. Paterson, *Phys. Rev. Lett.* **94**, 153901 (2005).
 [8] D. G. Grier, *Nature (London)* **424**, 810 (2003).
 [9] See for example: G. C. G. Berkhout and M. W. Beijersbergen, *Phys. Rev. Lett.* **101**, 100801 (2008); M. Harwit, *Astrophys. J.* **597**, 1266 (2003).
 [10] See for example: T. B. Leyser *et al.*, *Phys. Rev. Lett.* **102**, 065004 (2009); B. Thidé, *Phys. Rev. Lett.* **99**, 087701 (2007).
 [11] See for example: R. Marchiano and J.-L. Thomas, *Phys. Rev. Lett.* **101**, 064301 (2008); P. Z. Dashti, F. Alhassen, and H. P. Lee, *Phys. Rev. Lett.* **96**, 043604 (2006).
 [12] S. Sasaki and I. McNulty, *Phys. Rev. Lett.* **100**, 124801 (2008).
 [13] M. Uchida and A. Tonomura, *Nature (London)* **464**, 737 (2010).
 [14] See for example: S. Tung, V. Schweikhard, and E. A. Cornell, *Phys. Rev. Lett.* **97**, 240402 (2006); K. C. Wright *et al.*, *Phys. Rev. Lett.* **102**, 030405 (2009).
 [15] A. T. O’Neil *et al.*, *Phys. Rev. Lett.* **88**, 053601 (2002).
 [16] J. E. Curtis and D. G. Grier, *Phys. Rev. Lett.* **90**, 133901 (2003).
 [17] Y. Roichman *et al.*, *Phys. Rev. Lett.* **100**, 013602 (2008).
 [18] A. Niv *et al.*, *Opt. Lett.* **33**, 2910 (2008).
 [19] K. Miyakawa, H. Adachi, and Y. Inoue, *Appl. Phys. Lett.* **84**, 5440 (2004).
 [20] H. Adachi, S. Akahoshi, and K. Miyakawa, *Phys. Rev. A* **75**, 063409 (2007).
 [21] Y. Zhao *et al.*, *Phys. Rev. Lett.* **99**, 073901 (2007).
 [22] Q. Zhan, *Adv. Opt. Photon.* **1**, 1 (2009).
 [23] C. Maurer *et al.*, *New J. Phys.* **9**, 78 (2007).
 [24] X. L. Wang *et al.*, *Opt. Lett.* **32**, 3549 (2007).
 [25] X. L. Wang *et al.*, *Opt. Express* **18**, 10786 (2010).
 [26] E. Hasman *et al.*, *Prog. Opt.* **47**, 215 (2005).
 [27] K. S. Youngworth and T. G. Brown, *Opt. Express* **7**, 77 (2000).
 [28] Q. Zhan and J. Leges, *Opt. Express* **10**, 324 (2002).
 [29] R. Dorn, S. Quabis, and G. Leuchs, *Phys. Rev. Lett.* **91**, 233901 (2003).
 [30] E. Hasman *et al.*, *Appl. Phys. Lett.* **82**, 328 (2003).
 [31] G. Biener *et al.*, *Opt. Lett.* **30**, 1096 (2005).
 [32] K. Y. Bliokh *et al.*, *Opt. Express* **16**, 695 (2008).
 [33] A. Niv *et al.*, *Opt. Lett.* **30**, 2933 (2005).
 [34] M. Born and E. Wolf, *Principles of Optics* (Cambridge University Press, Cambridge, 1999), 7th ed.
 [35] See supplementary material at <http://link.aps.org/supplemental/10.1103/PhysRevLett.105.253602> for a movie of the motion of trapped particles around the ring focus. A direct link to this document may be found in the online article’s HTML reference section.
 [36] M. V. Berry, *J. Opt. A* **11**, 094001 (2009).